**LHCb Collaboration** LHCb 2000-049 PHYS
September 13, 2000

# Performance of the Electromagnetic Calorimeter for $\pi^0$ detection in Physics channels

**A. Jacholkowska**
Laboratoire de l'Accelerateur Lineaire (LAL),
Universite de Paris-Sud (ParisXI) and CERN
**I.Korolko**
ITEP(Moscow) and CERN

# 1 Introduction

The main purpose of the LHCb electromagnetic calorimeter is to trigger on electrons and photons at Level-0, and to reconstruct $\gamma$s and $\pi^0$s for physics analysis [1]. The following channels containing a $\pi^0$ from $\mathrm{B}_d^0$ decays have been studied:

- $\mathrm{B}_d^0 \to \pi^+\pi^-\pi^0$, which produces a high energy $\pi^0$ (up to 100 GeV). The theoretically predicted branching ratios vary between a few times $10^{-5}$ (for the $\rho^+\pi^-$ state) and a few times $10^{-6}$ (for the $\rho^0\pi^0$ state) [3] and [4]. The study of this channel allows extraction of the angle $\alpha$ of the unitarity triangle.
- $\mathrm{B}_d^0 \to \bar{D}^0\mathrm{K}^*$, where the $\bar{D}^0$ decays to $K^+\pi^-\pi^0$. In this channel $\pi^0$s are produced with medium energy of $\sim$ 10 GeV. The predicted branching ratios vary between $10^{-7}$ and $10^{-8}$[1]. This B decay mode allows the extraction of the angle $\gamma$ of the unitarity triangle.

The optimisation of the LHCb electromagnetic calorimeter granularity performed for the selected B decay modes is described in details in our previous note [6]. The reconstruction efficiency of energetic $\pi^0$s from $B_d^0 \to \pi^+\pi^-\pi^0$ reaction is limited by a fact that both decay photons often overlap and form the single cluster in the calorimeter. For softer $\pi^0$s from $B_d^0 \to \bar{D}^0\mathrm{K}^*$ reaction the pile-up effect (energy contributions from neighbour tracks) becomes more important.

# 2 $\pi^0$ detection in the $\mathrm{B}_d^0 \to \pi^+\pi^-\pi^0$ channel

## 2.1 selection and cuts

Full simulation studies on the selection of the $\mathrm{B}_d^0 \to \pi^+\pi^-\pi^0$ channel have been performed. The charged pions are reconstructed in the tracking devices and are identified in the RICH detectors. At present, only $\pi^0$s built from two resolved photons are used in the analysis.

The following selections and cuts have been applied on the studied sample:

- A preselection for charged pions and photons which required the momentum or energy to exceed a value which is dependent on the polar angle of the candidate respectively:
  $p_{\pi^\pm} > p(\theta)$ $(1 - 2\ \mathrm{GeV}/c)$ where $\theta$ is $\pi^\pm$ polar angle,
  $E_\gamma > E(\theta)$ $(2 - 6\ \mathrm{GeV})$,
  $\pi^0$ formed only from isolated clusters,
  $3\sigma$ cuts on invariant masses of $\pi^0$,$\rho$ and $\mathrm{B}_d^0$,
- Trigger L0 and L1 cuts,

Other analysis cuts related to the Dalitz plot cut, vertexing, tagging and discriminant estimator selection have been sudied elsewhere [4].

## 2.2 Results

Figure 1 presents the $\pi^0$ energy and emission angle $\theta$ compared to the generated true $\pi^0$ distributions in the $B_d^0 \to \pi^+\pi^-\pi^0$ channel. No kinematical cuts have been applied. As expected for the resolved $\pi^0$s the low energy ($E_{\pi^0}$ <2 GeV) and high energy ($E_{\pi^0}$ >80 GeV) are lost in the detector. A factor of 0.1 has been applied on the truth distributions.

The LHCb acceptance values are shown in table 1 for the $B_d^0 \to \rho^+\pi^-$ and in table 2 for the $B_d^0 \to \rho^0\pi^0$ candidates (normalized to the $4\pi$ acceptance). The present values are similar to those obtained in TP. An improuvement of the LHCb acceptance in the $\rho^+\pi^-$ channel reflects a better reconstruction efficiency for the medium energy $\pi^0$s. The other cuts refer to the L0 and L1 trigger selections. Only L0 trigger has been tunned to the present detector conditions. A 50% efficiency of the L0 trigger is lower by 10% with respect to the the $B_d^0 \to \pi^+\pi^-$ channel and a use of the $\pi^0$ trigger is under study [5].

| | $\varepsilon$(TDR) | $\varepsilon$(TP) |
|---|---|---|
| LHCb acceptance | 0.0135 | 0.009 |
| L0 efficiency | 0.51 | - |
| L0+L1 efficiency | 0.20 | - |
| L0+L1+L2+tag efficiency | 0.10 | 0.10 |
| Kinematical cuts efficiency | 0.60 | 0.60 |

Table 1: Reconstruction efficiencies for $B_d^0 \to \rho^+\pi^-$ channel.

| | $\varepsilon$(TDR) | $\varepsilon$(TP) |
|---|---|---|
| LHCb acceptance | 0.0125 | 0.0130 |
| L0 efficiency | 0.47 | - |
| L0+L1 efficiency | 0.18 | - |
| L0+L1+L2+tag efficiency | 0.09 | 0.13 |
| Kinematical cuts efficiency | 0.66 | 0.80 |

Table 2: Reconstruction efficiencies for $B_d^0 \to \rho^0\pi^0$ channel.

Figure 2 shows the two photon invariant mass in $B_d^0 \to \pi^+\pi^-\pi^0$ events, for photons with energy above 1 GeV. All photons, also from the primary vertex, are considered. Figure 3 shows the two photon invariant mass in $B_d^0 \to \pi^+\pi^-\pi^0$ events, both photons coming from the $B_d^0$ decay. The mean resolution on the $\pi^0$ mass is 6.7 MeV for in case of $\pi^0$ originating from the $B_d^0$ and 5.7 MeV for all $\pi^0$s also from the primary vertex fragmentation. These values are in good agreement with those quoted in the Technical Proposal (TP). After kinematical cuts, the overall efficiency for $\pi^0$ reconstruction is 20%, with a signal to combinatorial background ratio of approximately 1. The measured $\pi^0$ mass is used in further $B_d^0$ mass reconstruction.

Figure 4 shows the three $\pi$s invariant mass. After $3\sigma$ cut on $\pi^0$ mass the measured $B_d^0$ width is 42.0 MeV/$c^2$ (similar to the TP value).

An improuvement of 15% can be observed when using a constraint $\pi^0$ mass fit. The effect of the $\pi^0$ contribution to the $B_d^0$ width can be evaluated by setting the $\pi^0$ momentum vector components to their values at the generator level. With this "true" $\pi^0$ the $B_d^0$ width lowers to 14.5 MeV/$c^2$, below the value of 17.0 MeV/$c^2$ quoted in [2] for the $B_d^0 \to \pi^+\pi^-$ channel.

| mass resolution | $\sigma$(TDR) MeV | $\sigma$(TP) MeV |
|---|---|---|
| $\pi^0$ | 5.7 | 6.3 |
| $B_d^0$ | 42.0 | 44.4 |
| $B_d^0$ $\pi^0$ constraint fit | 35.7 | - |
| $B_d^0$ with true $\pi^0$ | 14.5 | - |

Table 3: Reconstruction resolution for $\pi^0$ and $B_d^0$.

The effect of the LHCb acceptance in the Dalitz plot (within applied kinematical cuts and $3\sigma$ cut on $B_d^0$ mass) can be evaluated when comparing figures 5 and 6.The overall loss factor due to acceptance and reconstruction of charged and neutral $\pi$s is 0.115.

## 2.3 Comparison with $B_d^0 \to \pi^+\pi^-$ channel

The annual event yields [2] for triggered, fully reconstructed and tagged events are :

$$\begin{array}{rl} \rho^+\pi^- & \sim 1000 \text{ (BR} = 44\times10^{-6}) \\ \rho^-\pi^+ & \sim 200 \text{ (BR} = 10\times10^{-6}) \\ \rho^0\pi^0 & \sim 100. \text{ (BR}= 1\times10^{-6}) \end{array}$$

The above branching fractions are crude theoretical estimations used in other studies of these decays [3]. The corresponding annual event yield for $B_d^0 \to \pi^+\pi^-$ is 4900 (with BR= $5\times10^{-6}$).

The loss factor of 50 compared to $B_d^0 \to \pi^+\pi^-$ channel may be decomposed into the following contributions:

the LHCb acceptance loss of ( $\sim$ 10.0) with respect to the $B_d^0 \to \pi^+\pi^-$ channel which acoounts for the factor of ( $\sim$ 3.0) for the $\gamma$ conversions and ( $\sim$ 3.3) for the resolved $\pi^0$ reconstruction , severe background suppression cuts and lower trigger efficiency leading to a factor of ( $\sim 5.0$). which splits into 3.1 and 1.5 average values.

The high loss factor could be decreased in future in several ways:

- considering the $\gamma$ conversions behind the magnet,
- reconstructing $\pi^0$ candidate from the overlapping $\gamma$ clusters,
- lowering the requirements for the background suppression (e.g. see effect of the $\pi^0$ constraint fit on $B_d^0$ width).

Simple estimation of these improvements related to the future reconstruction developments may bring a recovery of a factor of 5 to 10 in the $B_d^0 \to \pi^+\pi^-\pi^0$ reconstruction efficiency.

# 3 $\pi^0$ detection in the $B_d^0 \to \bar{D}^0 K^*$ channel

## 3.1 Motivations

The $B_d^0$ decay into $\bar{D}^0 K^*$ system provides a measurement of the angle $\gamma$ of the unitarity triangle. The full analysis procedure for this channel is described in [1] for final states with charged particles only. The physics performance is limited by very low visible branching ratios. Only ~340 events of the type $B_d^0 \to \bar{D}^0 K^*$ followed by $\bar{D}^0 \to K^+\pi^-$ (~50 $B_d^0 \to D^0 K^*$ events) are expected to be reconstructed in one year of data taking. This situation could be improved by adding the measurement of $\bar{D}^0 \to K^+\pi^-\pi^0$ ( and $D^0 \to K^-\pi^+\pi^0$) which benefits from higher (by a factor of $3.62 \pm 0.24$ [7]) branching ratio.

## 3.2 Results

The analysis was started by the preselection which requires all 4 charged particles (from $\bar{D}^0$ and $K^*$ decays) to be reconstructed in the spectrometer. The efficiency of such preselection is 8.2% (normalized to all events produced in $4\pi$). Figure 7 presents the transverse momentum spectrum of signal $\pi^0$s from preselected events.
Next, Monte-Carlo truth information was used to define a potentially reconstructible events requiring that:

1. both photons from the signal $\pi^0$ decay point to the calorimeter acceptance,
2. transverse momentum of each photon exceed $0.1 GeV/c$ and energy is greater than $1 GeV/c^2$. The last cut suppresses a small amount (about 5%) of extremely low energy $\pi^0$s close to the outer edge of the calorimeter.

A large fraction of preselected events (47.4%) satisfies these requirements.

Finally both photons were checked to be reconstructed in the calorimeter as two separated $3\times3$ cells neutral clusters. Only $\sim 28\%$ of potentially reconstructible events survive this last step. Low efficiency of $\pi^0$ reconstruction is explained by relatively large amount of material ($\sim 70\%$ of radiation length on average) between the interaction region and the calorimeter resulting in a high rate of photon conversion. Figure 8 shows the two photon invariant mass for fully reconstructed events. Fitting the central part of the distribution with a Gaussian the $\pi^0$ mass resolution was determined to be 6.7 MeV. The tail at high masses is explained by the pile-up from neighbour tracks.

Requiring the measured $\pi^0$ mass to be within $2\sigma$ from its nominal value the $\bar{D}^0$ meson was reconstructed with a mass resolution of $18.6MeV/c^2$ as shown in Figure 9. A kinematic fit with a $\pi^0$ mass constraint could considerably improve this result up to $13.2MeV/c^2$.

The $B_d^0$ mass distributions obtained after a $3\sigma$ cut on the $\bar{D}^0$ mass are shown in Figure 10:

- the $B_d^0$ mass obtained with a measured momenta of all particles (without any sub-mass constraints) is shown in the upper plot. The mass resolution is $29.4MeV/c^2$,

- the $B_d^0$ mass obtained after a kinematic fit with $\pi^0$ and $\bar{D}^0$ masses as constraints is shown in the lower plot. The mass resolution is $12.2MeV/c^2$.

The efficiencies of all successive steps of the analysis are summarised in table 4 (all normalized to events produced in $4\pi$).

| | Efficiency, $\varepsilon$ |
|---|---|
| all charged tracks reconstructed | 8.2 |
| photons point to the ECAL acceptance | 5.8 |
| $P_T > 0.1GeV/c$ and $E > 1GeV/c^2$ | 3.9 |
| both photons reconstructed | 1.1 |
| $\pi^0$ $2\sigma$ mass window | 0.80 |
| $\bar{D}^0$ $3\sigma$ mass window | 0.72 |

Table 4: Reconstruction efficiencies for $B_d^0 \rightarrow \bar{D}^0\mathrm{K}^*$ channel

The efficiency of high $P_T$ (Level0) and vertex (Level1) triggers determined for events which have passed through all steps of the analysis was found to be 21.5%. Assuming further reconstruction procedure to be the same as described in [1] the expected increase in the statistics for analysis of the $B_d^0 \rightarrow \bar{D}^0\mathrm{K}^*$ channel is about 30%. The main factor limiting the $\pi^0$ reconstruction efficiency (photon conversion) is well understood and could be decreased in future by including in the analysis events with photons converting behind the magnet. The combinatorial background is an important issue and has to be validated (work is in progress).

# References


[1] LHCb Technical Proposal, CERN/LHCC 98-4 (1998).

[2] Proceedings of the Workshop on SM physics (and more) at the LHC, CERN 2000-004, Bdecays (2000).

[3] The BaBar Physics Book, SLAC-R-504 (1998).

[4] A.Jacholkowska and J.F.Libby,
The measurement of CKM–angle $\alpha$ using decays $B_d^0 \to \pi^+\pi^-\pi^0$,
LHCb 2000-058 PHYS.

[5] Z.Ajaltouni, V.Breton, O.Deschamps, A.Falvard, P.Perret, and A.Ziad,
Proposal for a $\pi^0$ trigger at level-0, LHCb 2000-024.

[6] S.Barsuk, I.Belyaev, A.Golutvin, I.Korolko,
Optimization of cell sizes of electromagnetic calorimeter, LHCb CALO 1999-034.

[7] Particle Data Group, The European Physical Journal C3 (1998) 1.

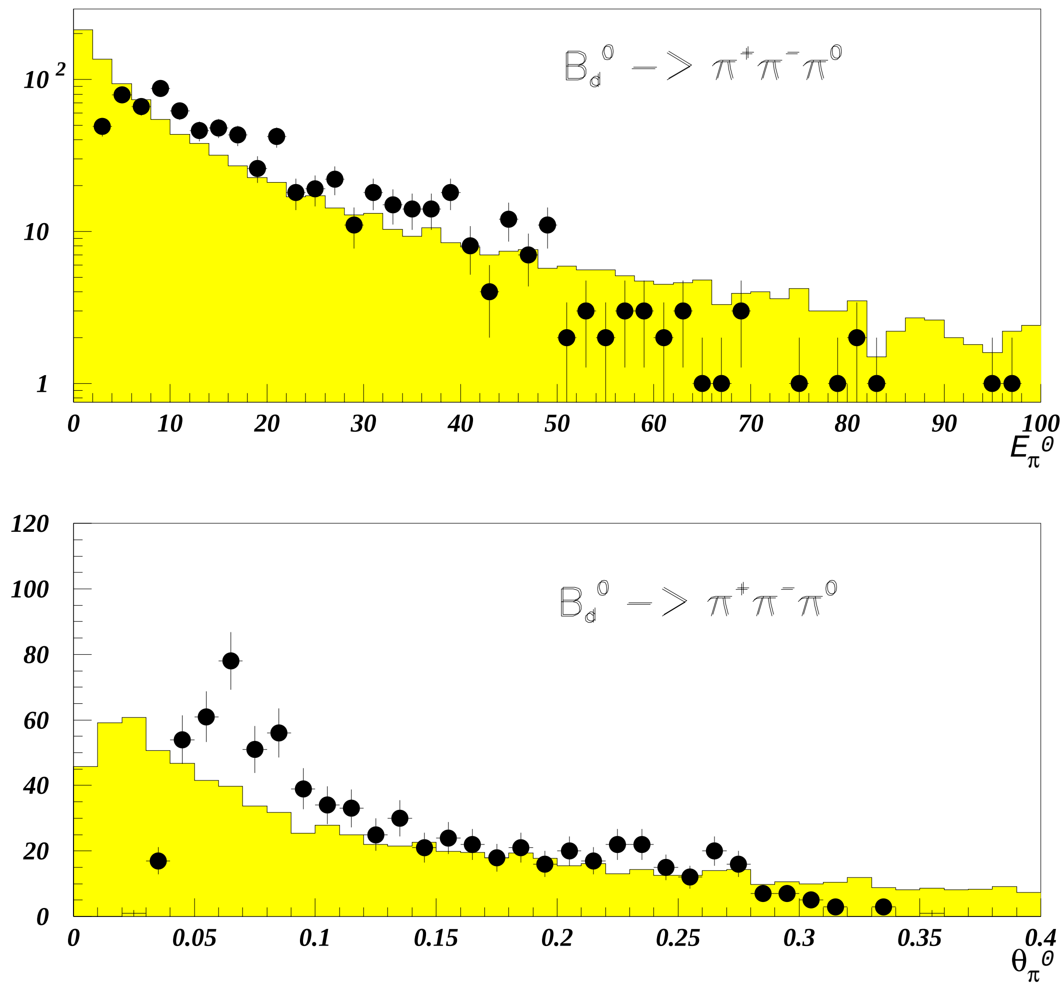


Figure 1: $E_{\pi^0}$ and $\theta_{\pi^0}$ in $B_d^0 \to \pi^+\pi^-\pi^0$ events compared to the generated $\pi^0$s energy and emission angle (full line). A factor of 0.1 was applied to the generated distribution.

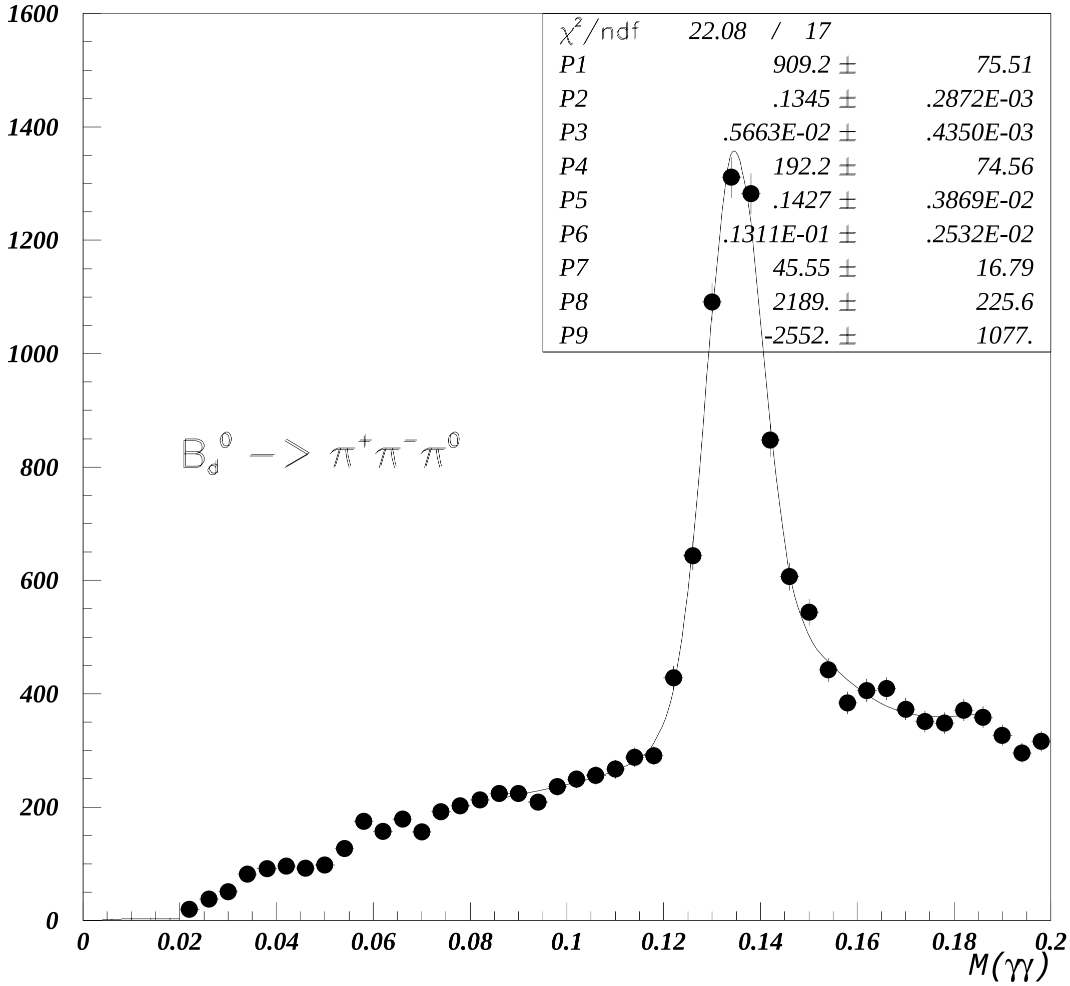


Figure 2: Reconstructed invariant mass for $\pi^0$ candidates in $B_d^0 \to \pi^+\pi^-\pi^0$ events in case when all $\pi^0$s (also from the primary fragmentation) are considered.

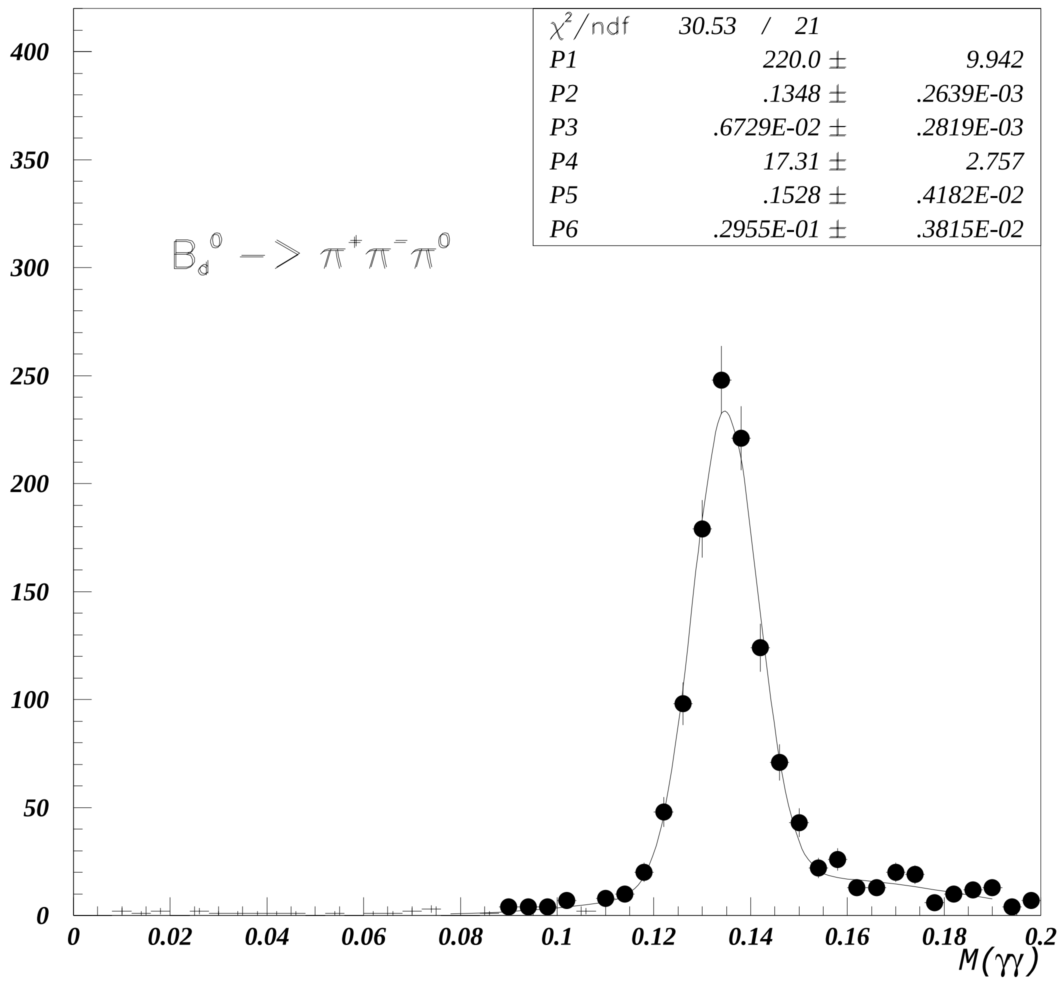


Figure 3: Reconstructed invariant mass for $\pi^0$ candidates in $B_d^0 \to \pi^+\pi^-\pi^0$ events, only for $\pi^0$ from $B_d^0$.

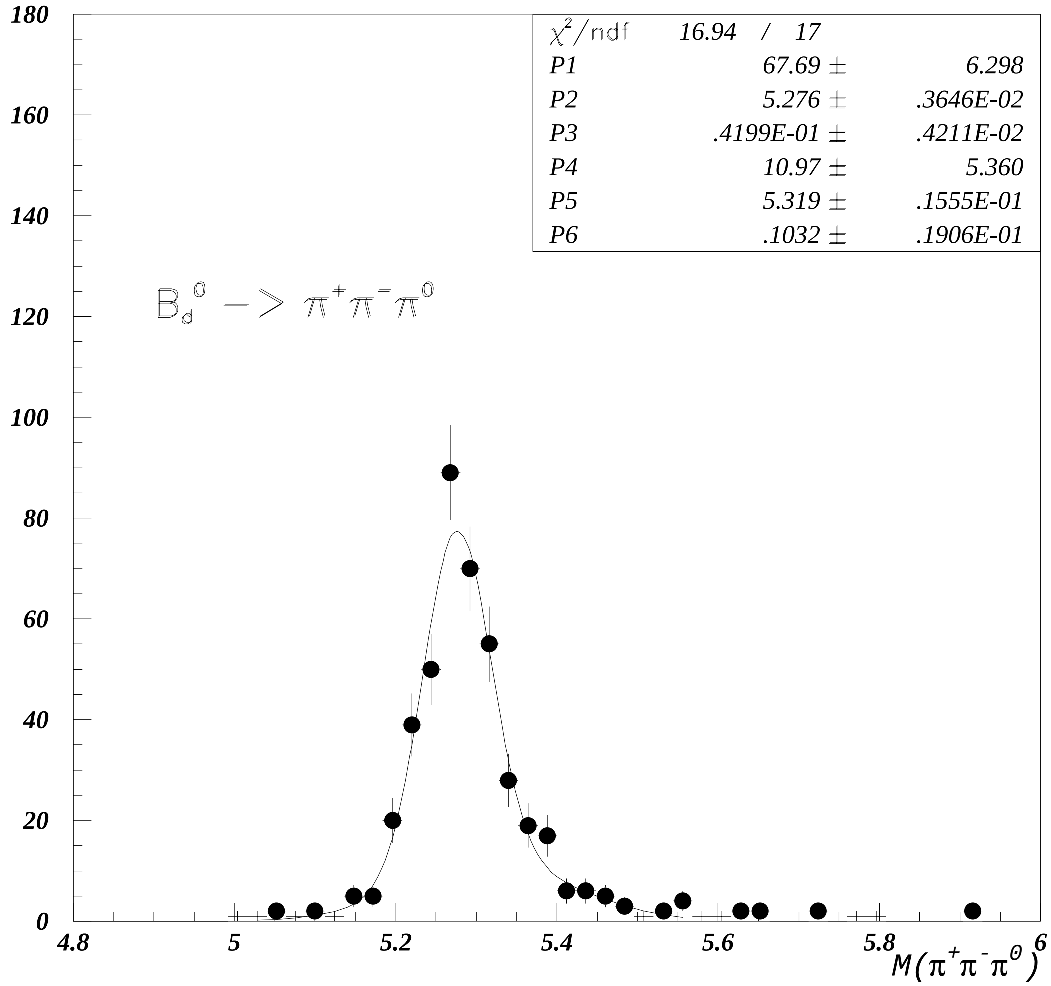


Figure 4: Reconstructed invariant mass of $\pi^+\pi^-\pi^0$ for $B_d^0 \rightarrow \pi^+\pi^-\pi^0$ candidates. A $3\sigma$ cut on $\pi^0$ mass has been applied.

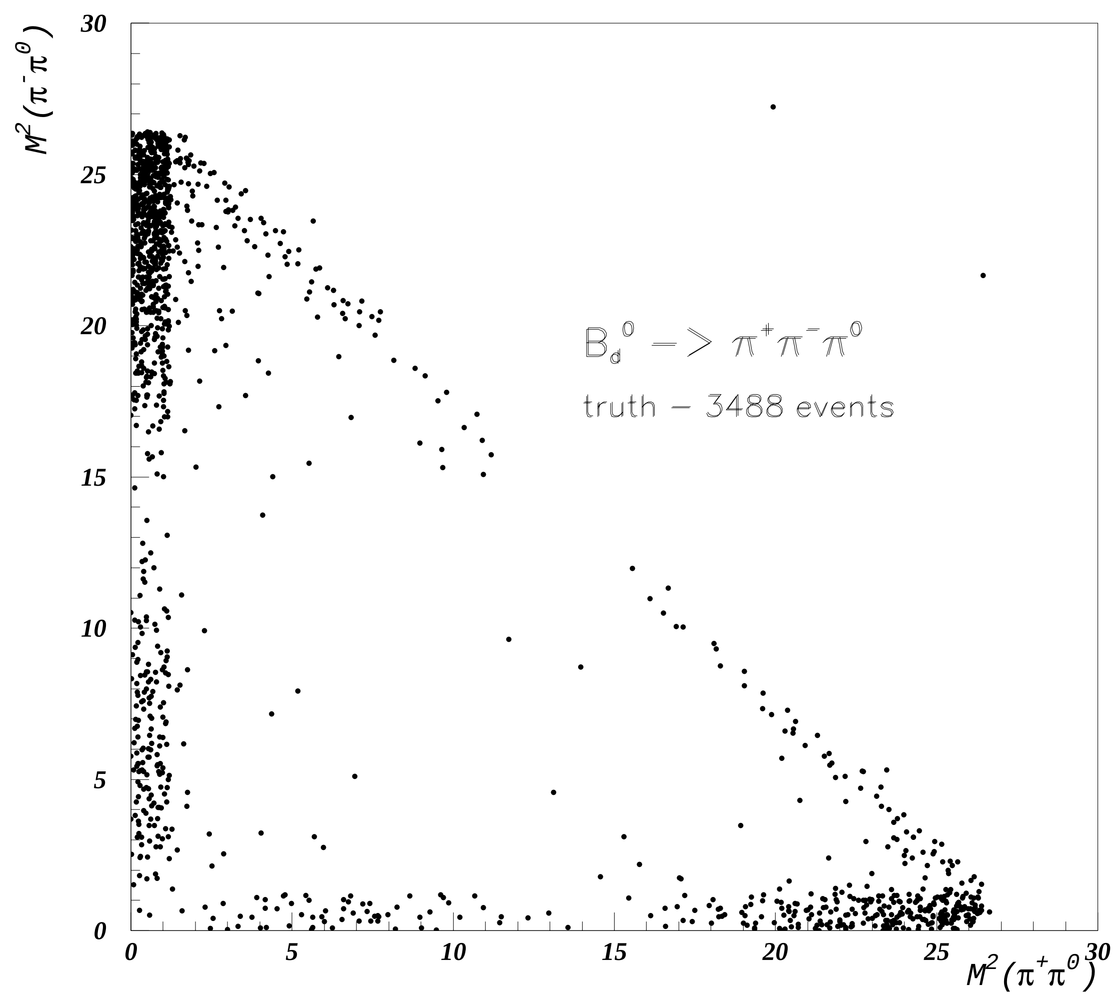


Figure 5: The Dalitz plot for $\mathrm{B}_d^0 \to \pi^+\pi^-\pi^0$ decays after kinematical (truth level) cuts.

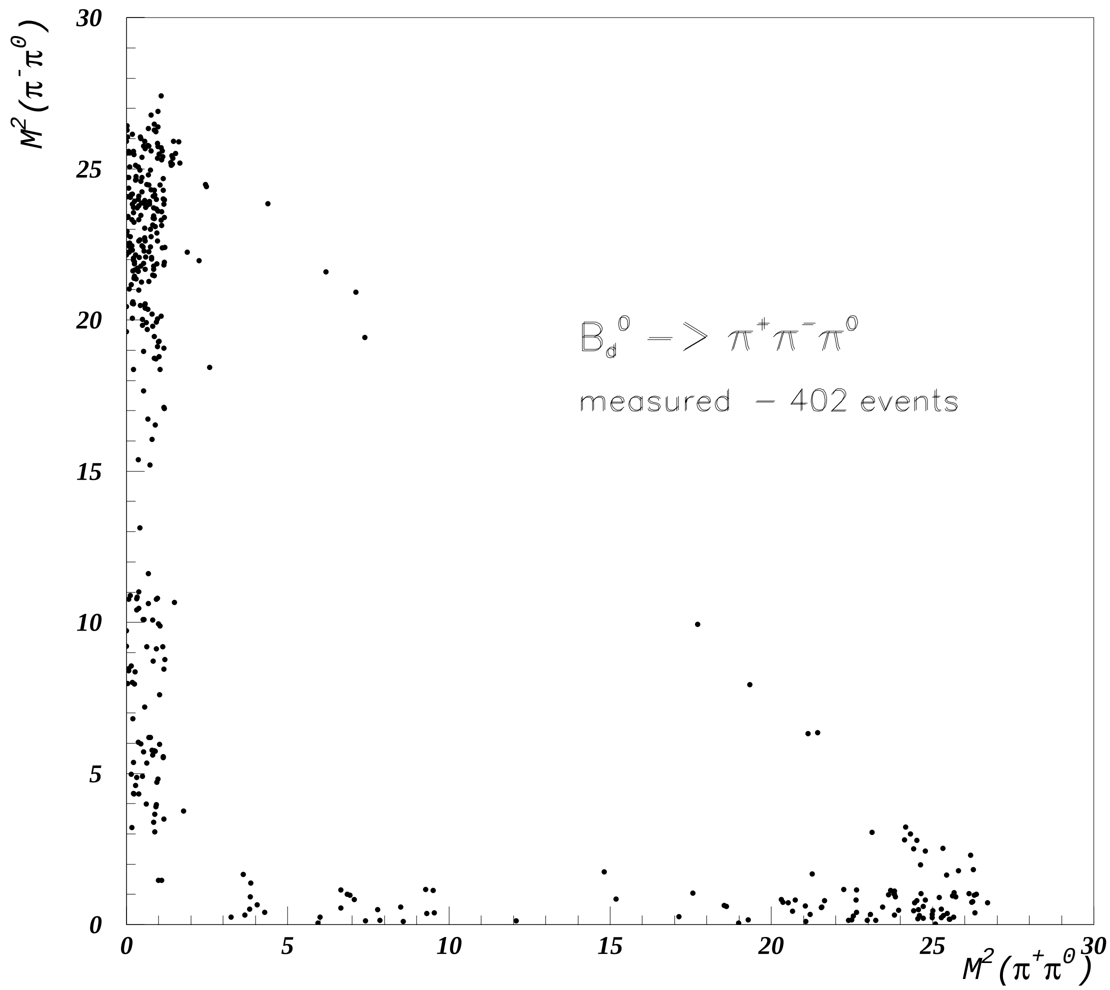


Figure 6: The Dalitz plot for $B_d^0 \to \pi^+\pi^-\pi^0$ decays after LHCb acceptance cuts and kinematical cuts.

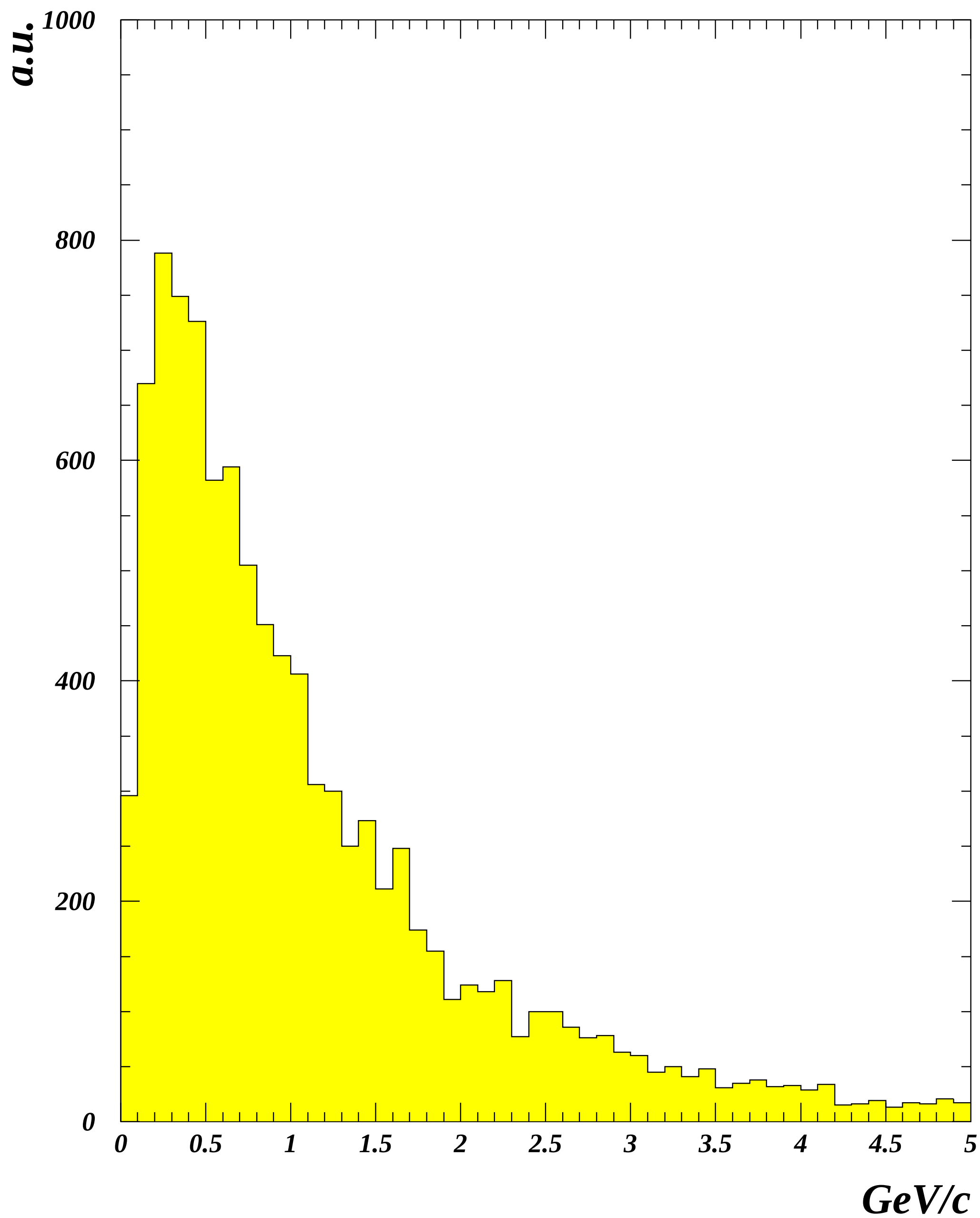


Figure 7: The $P_T$ spectrum of $\pi^0$s from preselected events.

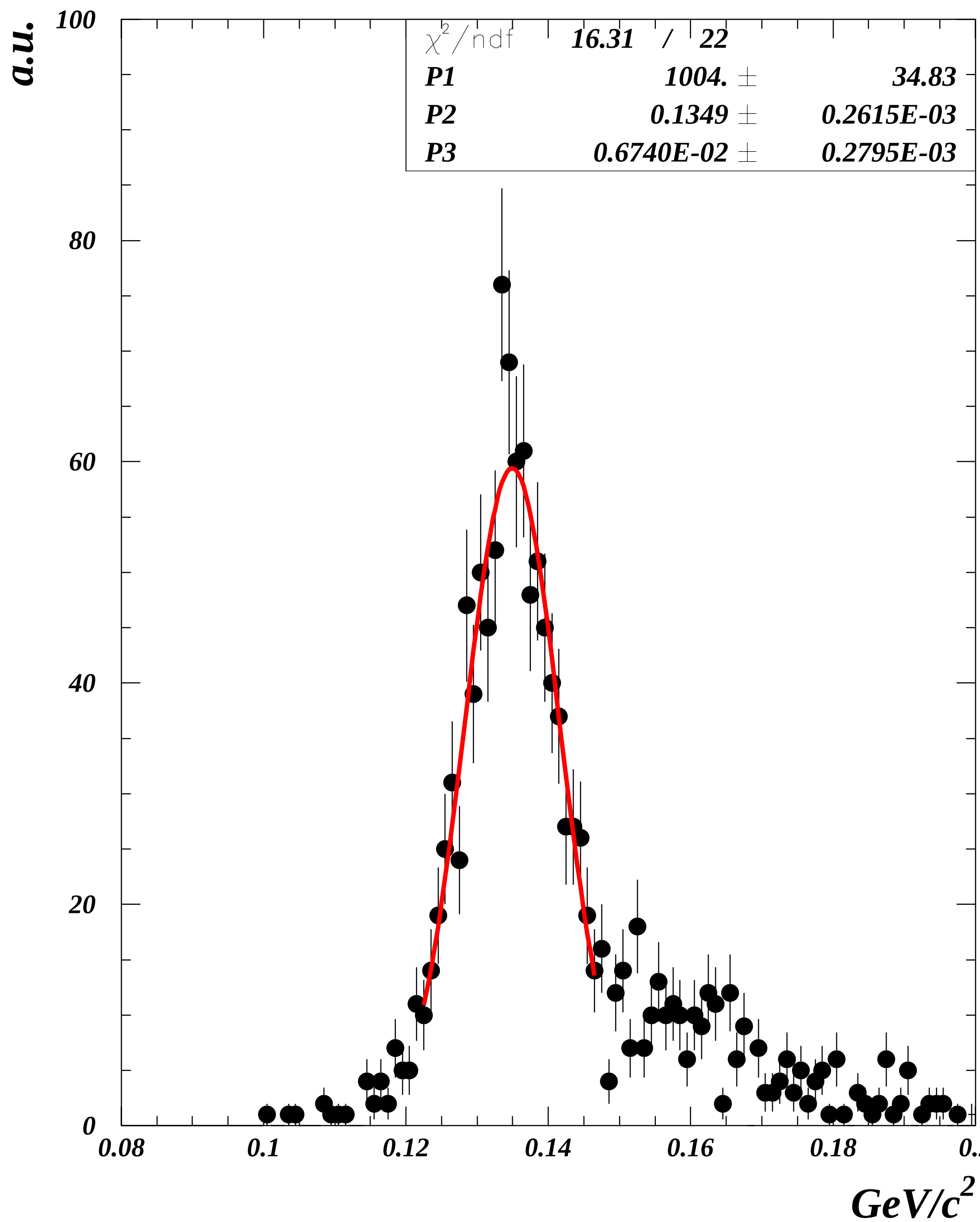


Figure 8: Reconstructed invariant mass for signal $\pi^0$s from $B_d^0 \to \bar{D}^0\mathrm{K}^*$ decays.

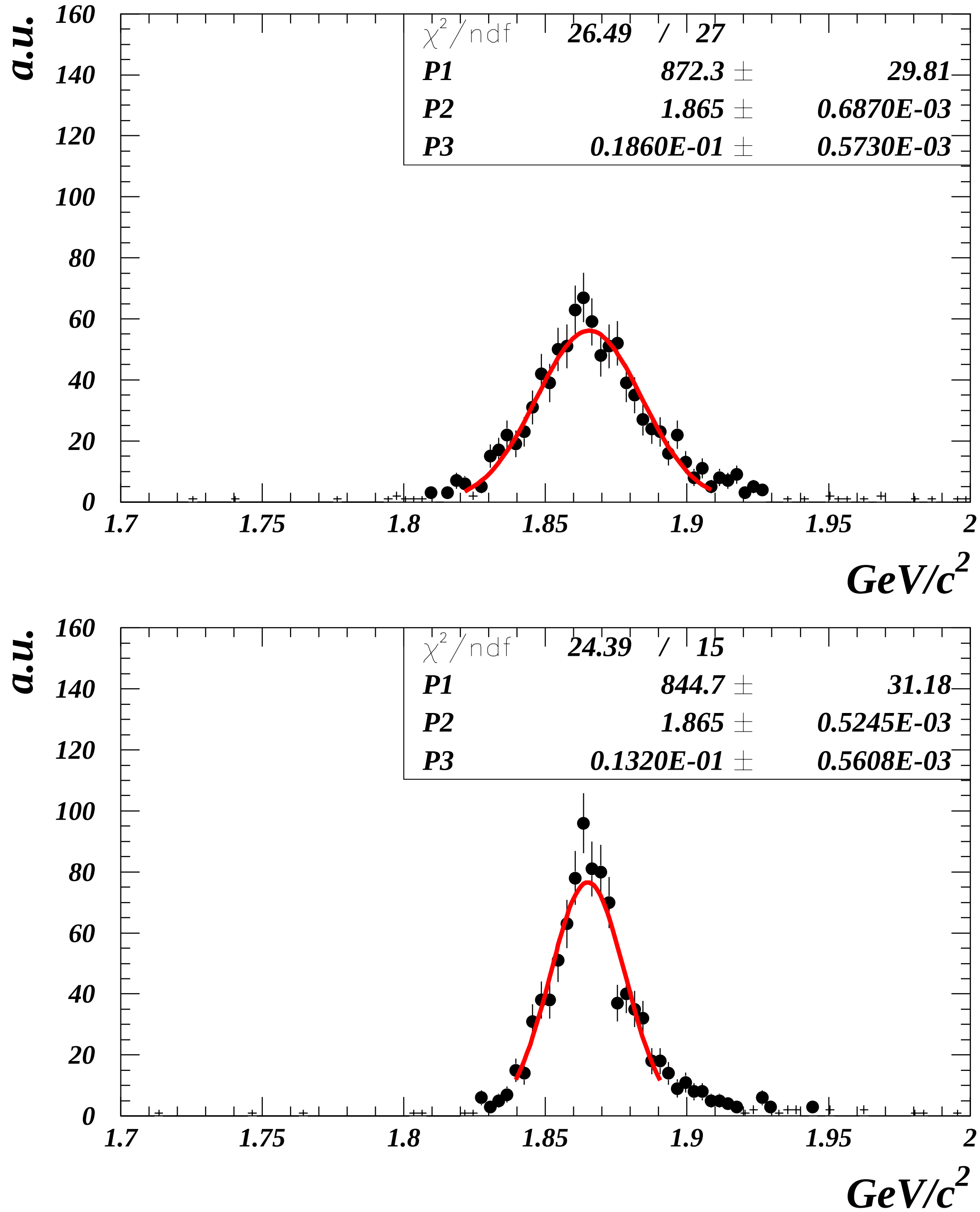


Figure 9: Reconstructed invariant mass of $K^+\pi^-\pi^0$ system after a $2\sigma$ cut on $\pi^0$ mass. Upper plot obbtained with measured momenta. Lower plot obtained after a kinematic fit with a $\pi^0$ mass constraint.

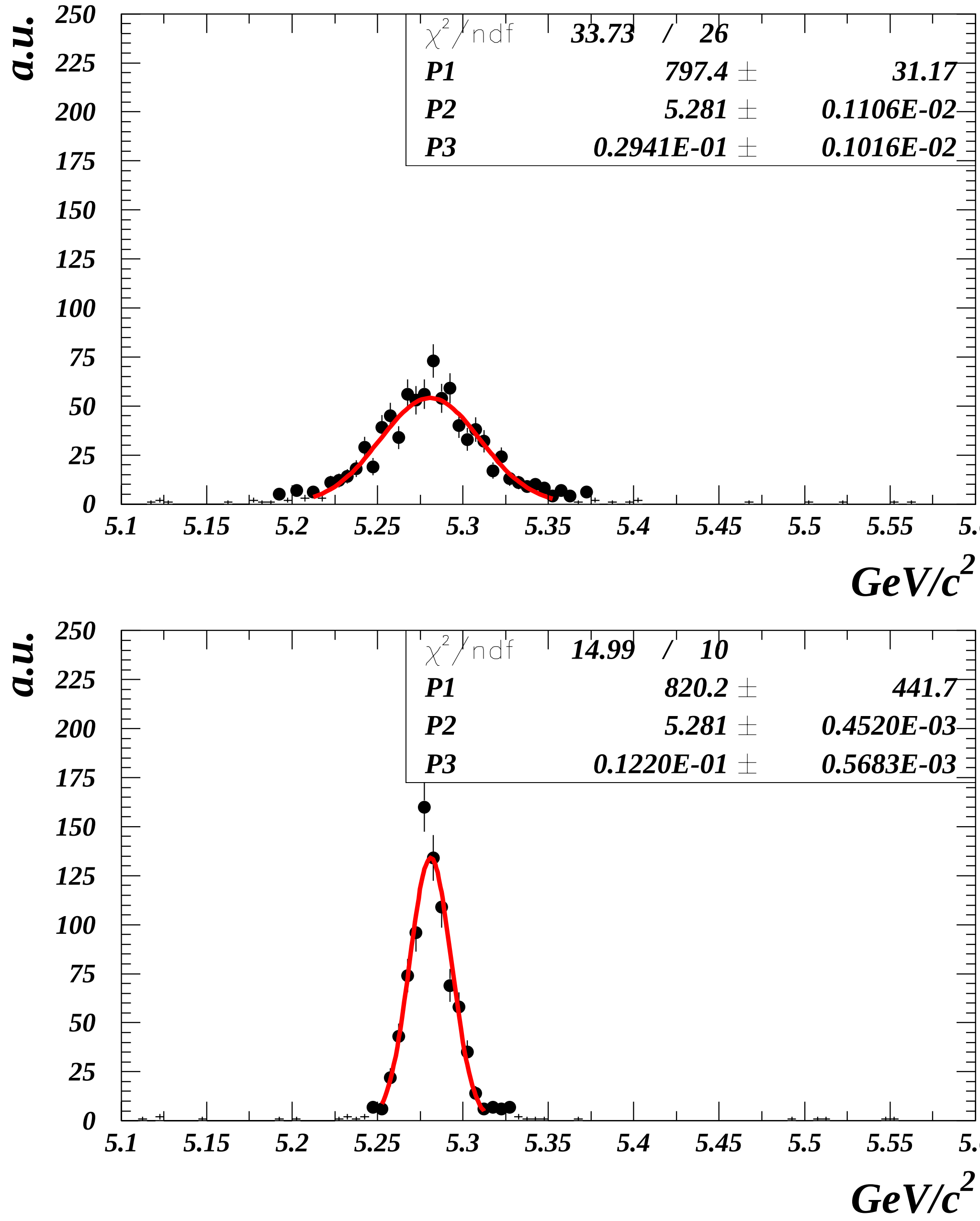


Figure 10: Reconstructed invariant mass of $B_d^0$ meson after a $3\sigma$ cut on $\bar{D}^0$ mass. Upper plot obbtained with measured momenta. Lower plot obtained after a kinematic fit with a $\pi^0$ and $\bar{D}^0$ mass constraints.